DOI: 10.1002/anie.200701028

Clathrates

$K_7B_7Si_{39}$, a Borosilicide with the Clathrate I Structure

Walter Jung, Josef Lörincz, Reiner Ramlau, Horst Borrmann, Yurii Prots, Frank Haarmann, Walter Schnelle, Ulrich Burkhardt, Michael Baitinger, and Yuri Grin**

The clathrate I type silicides of the alkali metals were first prepared by thermal decomposition of the monosilicides in 1948.[1] However, their crystal structures and the chemical composition M_8Si_{46} (M = Na, K) have been known only since 1965.[2] The compounds exhibit metallic electrical conductivity, because the valence electrons donated by the alkali-metal atoms are not required for the framework of four-bonded silicon atoms.[3] Partial substitution of silicon by trivalent atoms resulted in compounds such as $K_8Ga_8Si_{38}$ and $Rb_8Ga_8Si_{38}$. With the electronic balances $[K^+]_8[Ga^-]_8[Si^0]_{38}$ and $[Rb^+]_8[Ga^-]_8[Si^0]_{38}$, they follow the Zintl–Klemm concept and are semiconductors.[4] To date, the corresponding ternary clathrates with boron are not known. They are of special interest, however, because the substitution of silicon by boron results in a contraction of the clathrate framework. This contraction might facilitate the embedding of smaller cations into the cages. Such compounds are expected to be promising thermoelectric materials.[5]

$K_7B_7Si_{39}$ is the first borosilicide with a clathrate I crystal structure, and it has the smallest lattice parameter among all known clathrate compounds based on Group 14 elements. The compound can be obtained in the form of well-shaped crystals,[6] which is unusual, since the silicon clathrates are normally obtained as fine polycrystalline powders by thermal decomposition[1] or oxidation[7] of reactive starting compounds. Single crystals were prepared in only a few cases.[2,4,8,9]

The synthesis of $K_7B_7Si_{39}$ can be carried out by reaction of the elements in tantalum ampoules at approximately 900 °C; however, the conversion is not complete. The side products can be washed out, because $K_7B_7Si_{39}$ is stable towards sodium hydroxide solution as well as towards concentrated acids. Higher yields may be achieved if silicon and boron are allowed to pre-react in an arc melter.

Energy-dispersive X-ray spectroscopy (EDXS) investigations of $K_7B_7Si_{39}$ were performed in both scanning and transmission electron microscopes. The presence of boron was demonstrated qualitatively; potassium and silicon were found in a ratio of approximately 7:41, which is close to the expected ratio of 7:39.[10] Microcrystallites that clearly represented the clathrate phase (as demonstrated by selected area electron diffraction (SAED) and high-resolution transmission electron microscopy (HRTEM)) were analyzed by electron energy loss spectroscopy (EELS) in the regions of the fracture edges (thickness less than 10 nm). The experimental EEL spectrum (Figure 1) agrees well with that simulated for the composition $K_7B_7Si_{39}$ and a sample thickness of 5–10 nm. The composition determined by means of the crystal structure analysis was thus confirmed within the estimated standard deviations.

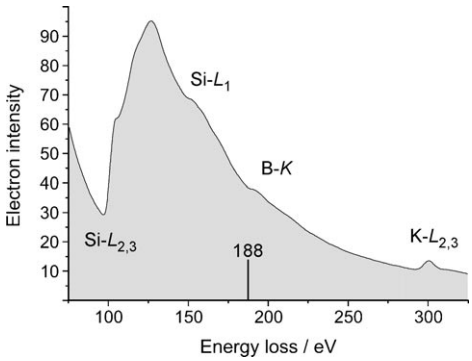

Figure 1. EEL spectrum of $K_7B_7Si_{39}$. Microcrystallite of $K_7B_7Si_{39}$ in the [111] orientation, boron *K* edge at 188 eV.

Metallographic investigation of polished single crystals confirmed the single-phase character of the material. However, some larger crystals showed inclusions in their nuclei (volume share less than 10%) which, according to EDXS analysis, do not contain potassium and which do not appear in the diffraction pattern. The total content of these phases in the sample is very low. The Guinier powder diffraction pattern can be indexed with a cubic lattice and a lattice parameter of $a = 9.952(1)$ Å. For samples with higher silicon content, the clathrate structure appears with larger lattice parameters up to $a = 9.971(1)$ Å. On the other hand, an increase of the boron content does not reduce the lattice parameter. This suggests a small homogeneity range stretching from $K_7B_7Si_{39}$ to higher Si:B ratios. For the binary phase $K_{7.0(1)}Si_{46}$, the lattice parameter is clearly larger (10.278(1) Å).[11]

The composition $K_7B_7Si_{39}$ was mainly established from the crystal structure determination with single-crystal X-ray diffraction data. According to this analysis, four-bonded

[*] Prof. Dr. W. Jung, J. Lörincz
Institut für Anorganische Chemie
Universität zu Köln
Greinstrasse 6, 50939 Köln (Germany)
Fax: (+49) 221-470-5083
E-mail: walter.jung@uni-koeln.de
R. Ramlau, H. Borrmann, Yu. Prots, F. Haarmann, W. Schnelle, U. Burkhardt, M. Baitinger, Prof. Dr. Yu. Grin
Max-Planck-Institut für Chemische Physik fester Stoffe
Nöthnitzer Straße 40, 01187 Dresden (Germany)
Fax: (+49) 351-4646-4001
E-mail: grin@cpfs.mpg.de

Supporting information for this article is available on the WWW under http://www.angewandte.org or from the author.

silicon and boron atoms form the framework of the clathrate I structure (space group $Pm\bar{3}n$) with tetracaidecahedral and pentagonal dodecahedral cavities (Figure 2). The structure refinement reveals that the former are fully occupied by

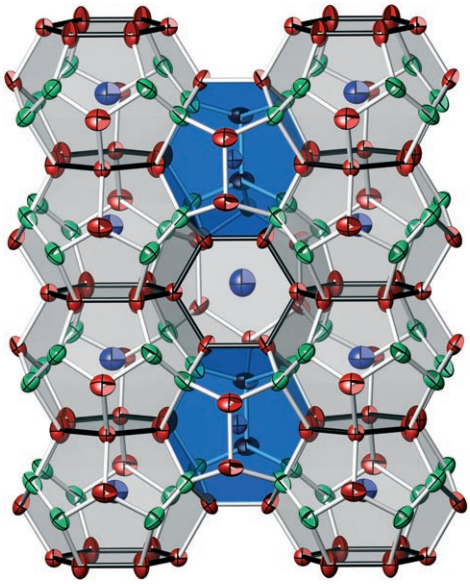

Figure 2. Crystal structure of $K_7B_7Si_{39}$ projected approximately along [100]. Split positions are not shown (see text). Green: (Si + B) on 16*i*, red: Si on 24*k* and 6*c*, blue: K on 2*a* and 6*d*. Pentagonal dodecahedra are shown in blue, the tetracaidecahedra in grey.

potassium atoms (site 6*d*) while the latter are only half-occupied (site 2*a*). The silicon atoms on site 16*i* (Figure 2, green) are partly substituted by boron atoms. However, on the sites 6*c* and 24*k*, only silicon atoms are found. This finding is remarkable, because in all known substitution and defect variants of the clathrate I structure, the vacancies or substituting atoms are located on the 6*c* site. A reason for this arrangement could be that, in contrast to the diamond structure of α-Si, the clathrate I structure contains planar six-membered rings in the tetracaidecahedra (highlighted by dark lines in Figure 2). These rings are only formed by atoms on the 6*c* and 24*h* sites with bond angles deviating considerably from those of a regular tetrahedron. The induced stress can be reduced either by substitution of silicon atoms on the 6*c* site by larger atoms with a lower tendency to form directed bonds (e.g. Ga,[4] Ni[12]) or by vacancies.[13] The smaller boron atoms, however, are expected to increase the stress. This analysis holds especially for atoms on the 6*c* site, because they participate in two planar six-membered rings. In return, the bond angles for the 16*i* site are very close to the tetrahedral ones, making this position especially suitable for boron.

For a precise determination of the composition and the crystal structure, the diffraction intensities were measured up to high angles ($Ag_{K\alpha}$ radiation, $2\theta_{max} = 98°$). Assuming that the Si/B position 16*i* is fully occupied, the refinement converges at an occupation of 6.8(3) B + 9.2 Si for this site and the composition $K_{7.04(2)}B_{6.8(3)}Si_{39.2(3)}$, or, in idealized form, $K_7B_7Si_{39}$. Owing to the size difference between boron and silicon atoms, the substitution leads to a spatial shift, and at the 16*i* site, split positions have to be considered. The two 16*i* positions (B + Si) are denoted as a and b in the structure fragment in Figure 3. Moreover, each original 24*k* site is substituted by three close neighboring positions c (24*k*) and

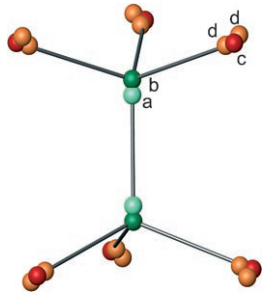

Figure 3. Key fragment of the Si–B framework with split position atoms *a*, *b* = 16*i* (7 B + 9 Si), *c* = 24*k* (Si), and *d* = 48*l* (Si).

2 × d (48*l*). The latter are oriented towards the boron positions. The structure determination reveals only the number of scattering electrons but not the distribution of the silicon and boron atoms on the 16*i* split positions. The a–a distance of 1.810 Å is observed for B–B bonds in metal borides, whereas the a–b distance of 2.057 Å corresponds to a B–Si bond and the b–b distance of 2.303 Å to a Si–Si bond. Locally, the occupation of the c or d positions by a silicon atom depends on which site (a or b) the neighboring Si or B atoms occupy. The (a, b)–(c, d) distances between 2.079 and 2.420 Å should be understood as B–Si and Si–Si bonds.

In the clathrate I compounds $Ba_8Ge_{43}\square_3$[14] and $Rb_8Sn_{44}\square_2$,[15] a 2 × 2 × 2 superstructure in the subgroup $Ia\bar{3}d$ was observed. For $K_7B_7Si_{39}$, neither X-ray diffraction on single crystals nor electron diffraction on microcrystallites[16] reveal the presence of a superstructure.

Defocusing series of HRTEM patterns were obtained in the orientations along [100], [110], and [111]. No hints of an ordering of the vacancies on the potassium position 2*a* or of the boron atoms on 16*i* were found. The defocusing series were simulated on the basis of a random distribution of the vacancies and the boron atoms, and these simulations agree very well with the experimental data (Figure 4).

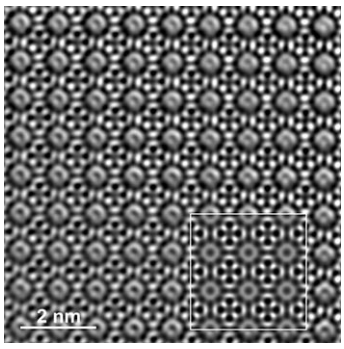

Figure 4. HRTEM image of $K_7Si_7B_{39}$ in the [100] orientation. A simulated image is shown in the inset, lower right (crystal thickness 5 nm, defocus −50 nm).

Evidence for the presence of structurally different boron atoms in $K_7B_7Si_{39}$ was obtained with solid-state NMR spectroscopy. The ^{11}B NMR signal ($I_{max}\delta = -5$ ppm) shows a shoulder towards higher frequencies (Figure 5a). Satellite

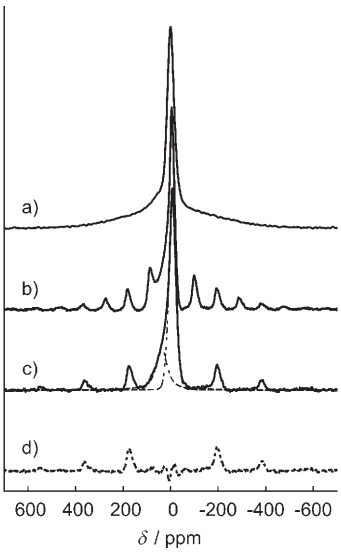

Figure 5. ^{11}B NMR spectra of $K_7B_7Si_{39}$: a) without sample rotation; b) rotation frequency of 15 kHz; c) rotation frequency of 30 kHz (the dashed lines represent the contributions of different boron atoms); d) subtraction of the simulated spectrum of the central transition from the MAS spectrum with 30 kHz.

transitions form a wide, unstructured contribution, because the coupling constants of the ^{11}B atoms vary owing to different local environments of the boron atoms. No further signals in the region ± 1 MHz around the central transition were found. In combination with the narrow central transition (full-width-at-half-maximum = 38 ppm), this finding shows that the signal is only moderately influenced by the quadrupole interaction (^{11}B nuclear spin $I = 3/2$). In the magic-angle spinning (MAS) experiment, all rotation bands were fully separated from the central transition at a rotation frequency of 30 kHz (Figure 5c).

The shoulder, which is clearly visible on the high-frequency side of the signal of the central transition, confirms the presence of structurally different boron atoms (Figure 5b,c). These differences might be caused either by the vacancies on the potassium position 2*a* or by the appearance of B–B bonds together with Si–B bonds. The intensity of the second signal is too large to be explained by the presence of boron-containing impurity phases. The equilibrium magnetization is achieved after 60 s, which is clearly longer than the relaxation time for a material with metallic conductivity.

$K_7B_7Si_{39}$ is diamagnetic. The magnetic susceptibility ($\chi(300\,K) \approx -250 \times 10^{-6}\,emu\,mol^{-1}$) is weakly temperature dependent. Accounting for small contributions from para- and ferromagnetic impurities, it can be expressed as $\chi(T) = \chi_0 + \chi_1 T$ ($\chi_0 = -180 \times 10^{-6}\,emu\,mol^{-1}$ and $\chi_1 = -0.29 \times 10^{-6}\,emu\,mol^{-1}\,K^{-1}$). The resistivity $\rho(T)$ is relatively large and increases with decreasing temperature.[17] The room-temperature value (ca. 3 mΩ m) is approximately doubled at 4 K. These observations are characteristic of a heavily doped semiconductor. This result can be easily understood in comparison with the calculated electronic density of states (Figure 6). For the calculation within density functional

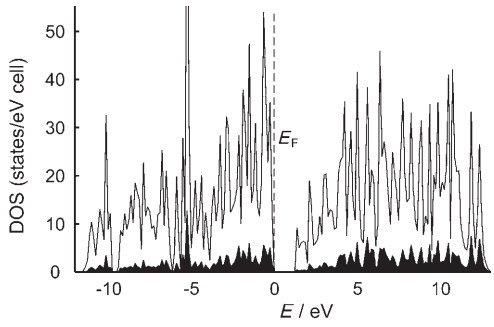

Figure 6. Electronic density of states (DOS) for a $K_8B_8Si_{38}$ model structure. The partial DOS for the boron atoms is shown in solid black.

theory,[18] a hypothetical ordering model $K_8B_8Si_{38}$ in the subgroup $P\bar{4}3n$ was created. Therein, the site 16*i* from the space group $Pm\bar{3}n$ splits up into two eight-fold sites, one of which is occupied by boron atoms. Both the model compound and $K_7B_7Si_{39}$ are in agreement with the Zintl–Klemm concept. As expected, a small value for the density of states at the Fermi level E_F is calculated, which agrees well with the behavior of the electrical resistivity.

The observed electronic transport properties agree with the long relaxation time in the NMR experiments. This behavior supports the results of the crystal structure determination, thus revealing equal numbers of boron and potassium atoms, which allows $K_7B_7Si_{39}$ to be interpreted as a Zintl phase. According to the lattice parameters, this composition represents the boron-rich border of a narrow homogeneity range. Crystal structure investigations and physical property measurements on phases with larger lattice parameters (and a higher Si:B ratio) are currently in progress. The smaller cages in boron-substituted clathrates may open a new perspective for the preparation of clathrate compounds with smaller cations, which are very rare to date.

Experimental Section

Synthesis: For the preparation of a single-phase product with the composition $K_7B_7Si_{39}$, a mixture of boron and silicon in a molar ratio of 8:38 was arc-melted and finely ground in a boron carbide mortar. The product was mixed with an excess of potassium (molar ratio K/Si/B = 12:38:8, total mass ca. 1 g) in an argon-filled glovebox and sealed under argon in a tantalum ampoule (outer diameter 10 mm, inner diameter 8 mm, length 40 mm). The ampoule, enclosed in a silica tube, was heated to 650 °C for one day, then heated to 900 °C at a rate of 10 °C h^{-1} and held at this temperature for two days. After homogenization under argon, the reaction product was treated two more days at 900 °C in a tantalum ampoule (sealed in a silica tube). The sample thus obtained contained some silicon and further unidentified products. These impurities were removed by washing with ethanol, aqua regia, hydrofluoric acid, and, finally, with sodium hydroxide solution. After this treatment, a well-crystallized clathrate was obtained as a single phase, as judged by X-ray powder diffraction.

Using amorphous or finely ground crystalline boron, the target phase $K_7B_7Si_{39}$ can also be prepared directly from the elements. However, these products showed lower purity.

Crystallographic data:[19] $K_7B_7Si_{39}$, $M_r = 1443.51$, cubic, space group $Pm\bar{3}n$, $a = 9.952(1)$ Å, $Z = 1$, $\rho_{calcd} = 2.434\ g\,cm^{-3}$, lattice parameter from powder X-ray diffraction (Huber Image Plate Guinier camera G670, $Cu_{K\alpha 1}$ radiation, $\lambda = 1.54056$ Å, LaB_6 as internal standard). Single crystal diffraction experiment: RIGAKU Spider diffractometer with rotating anode and Varimax optics, $Ag_{K\alpha}$ radiation, $\lambda = 0.56087$ Å, ω scans, $2\theta_{max} = 98°$, 21526 measured, 1845 independent, and 1238 observed ($F > 4\sigma(F)$) reflections. Absorption correction was performed by a multiscan procedure. Crystal structure refinement was made on F with the program package WinCSD:[20] 28 parameters refined, $R(F) = 0.116$, $R(F^2) = 0.060$. 1 K at 2*a*, 000, $B_{eq} = 0.49(2)$, *occ.* = 0.52(1); 6 K at 6*d*, 1/4 1/2 0, $B_{eq} = 1.50(2)$; 6 Si at 6*c*, 1/4 0 1/2, $B_{eq} = 0.46(2)$; 6.8(3) B + 9.2 Si at the split positions 2 × 16*i*, *xxx* $x_1 = 0.1828(2)$, $B_{eq} = 0.49(2)$, *occ.* B: 0.213(9), + Si: 0.287(9) and $x_2 = 0.1974(2)$, $B_{eq} = 0.40(2)$, *occ.* B: 0.212(9), + Si: 0.288(9); 24 Si at the split positions 24*k*, 0*yz*, $y = 0.1159(4)$, $z = 0.3069(4)$, $B_{eq} = 0.49(5)$, *occ.* = 0.32(1) and 48*l*, *xyz*, $x = 0.0145(2)$, $y = 0.1252(2)$, $z = 0.2924(2)$, $B_{eq} = 0.51(3)$, *occ.* = 0.347(3). Further details of the crystal structure determination may be obtained from the Fachinformationszentrum Karlsruhe, 76344 Eggenstein-Leopoldshafen (Fax: (+49) 7247-808-666, E-mail@fiz-karlsruhe.de), reference number CSD-418183.

Electron microscopy: For SAED, HRTEM, EDXS, and EELS, a Tecnai G2-F30 (FEI) electron microscope with a supertwin lens was operated at 300 kV. The setup was equipped with an energy filter GIF2001 (Gatan) and a US1000 CCD camera (Gatan). The samples were crushed in an agate mortar, dispersed in *n*-butanol, and put on a carbon-hole film. For simulation of the HRTEM images, the program package EMS (multislice formalism) was applied.[21] 25 EEL spectra on six crystallites were measured (diffraction modus) in the [100] and [111] orientations as well as on unoriented crystallites. The convergence angle of the incident beam was 1.1 mrad, the spectrometer collection angle was 4.9 mrad, the resolution of the spectrometer (measured as the half-width of the zero-loss peak) 0.75 eV, and the dispersion of the spectrometer 0.3 eV per pixel. For the simulation of the EEL spectra, the program "EELS Advisor" (Gatan) was used.[22] For EDXS on SEM, a Phillips XL 40 instrument and an EDAX detector with an ultrathin window for detection of light elements up to and including boron was employed.

Magnetization and electrical resistivity: Magnetization of a polycrystalline sample of $K_7B_7Si_{39}$ ($m \approx 86$ mg) was measured in a SQUID magnetometer (MPMS-XL7) in fields $\mu_0 H$ from 0.01 to 7 T. Electrical resistivity was measured with a DC four-point method on a cold-pressed parallelepipedal polycrystalline sample. The uncertainty of the absolute value is ±20%.

NMR spectroscopy: The experiments were performed with a Bruker AVANCE 500 WB spectrometer in a field of $\mu_0 H = 11.74$ T. The resonance frequency for ^{11}B in this field is 160.462 MHz. The chemical shift of the signals was referenced to $BF_3 \times OEt_2$. For measurements without rotation, a probe was used that is optimized for broad signals (NMR-Service, Erfurt). For MAS measurements, a standard CP-MAS probe was used (Bruker, Rheinstetten) as well as a ZrO_2 rotor (diameter = 2.5 mm). The spectra were registered with an echo-pulse sequence and pulses of equal duration. The MAS experiments were performed with rotor synchronization using an interpulse delay of $\tau = 1/\nu_{rot}$. For comparison of the line shapes, the spectra without rotation were registered with the same delay between the $\pi/2$ pulses. The duration of a $\pi/2$ pulse was 2 μs. Intensity measurements show that the equilibrium magnetization is achieved after about 60 s; thus, this time was chosen as the scan interval.

Received: March 7, 2007
Published online: August 2, 2007

Keywords: boron · clathrates · inclusion compounds · silicon · Zintl phases

[1] a) E. Hohmann, *Z. Anorg. Allg. Chem.* **1948**, *257*, 113–126; b) R. Schäfer, W. Klemm, *Z. Anorg. Allg. Chem.* **1961**, *312*, 214–220.
[2] a) J. Kasper, P. Hagenmuller, M. Pouchard, C. Cros, *Science* **1965**, *150*, 1713–1714; b) C. Cros, M. Pouchard, P. Hagenmuller, *C. R. Acad. Sci. Paris* **1965**, *260*, 4764–4767; c) J. Gallmeier, H. Schaefer, A. Weiss, *Z. Naturforsch. B* **1967**, *22*, 1080.
[3] a) G. K. Ramachandran, P. F. McMillan, J. Dong, O. F. Sankey, *J. Solid State Chem.* **2000**, *154*, 626–634; b) A. Moewes, E. Z. Kurmaev, J. S. Tse, M. Geshi, M. J. Ferguson, V. A. Trofimova, Y. M. Yarmoshenko, *Phys. Rev. B* **2002**, *65*, 153106.
[4] a) R. Kröner, K. Peters, H. G. von Schnering, R. Nesper, *Z. Kristallogr. New Cryst. Struct.* **1998**, *213*, 667–668; b) H. G. von Schnering, R. Kröner, H. Menke, K. Peters, *Z. Kristallogr. New Cryst. Struct.* **1998**, *213*, 677–678.
[5] J. L. Cohn, G. S. Nolas, V. Fessatidis, T. H. Metcalf, G. A. Slack, *Phys. Rev. Lett.* **1999**, *82*, 779–782.
[6] Supporting Information S1: REM pattern of $K_7B_7Si_{39}$ crystals.
[7] B. Böhme, A. Guloy, Z. Tang, W. Schnelle, U. Burkhardt, M. Baitinger, Y. Grin, *J. Am. Chem. Soc.* **2007**, *129*, 5348–5349.
[8] H. Fukuoka, J. Kiyoto, S. Yamanaka, *J. Solid State Chem.* **2003**, *175*, 237–244.
[9] M. Baitinger, J.-H. Chang, K. Peters, H. G. von Schnering, Y. Grin, *Z. Kristallogr. New Cryst. Struct.*, DOI: DOI: 10.1524/ncrs.20070035.
[10] Supporting Information S2: EDXS spectrum of the single crystal of $K_7B_7Si_{39}$ used for crystal structure analysis.
[11] Supporting Information S3: lattice parameters of silicides with the clathrate I crystal structure.
[12] G. Cordier, P. Woll, *J. Less-Common Met.* **1991**, *169*, 291–302.
[13] J. Llanos, Dissertation, Universität Stuttgart **1984**.
[14] a) R. F. W. Herrmann, K. Tanigaki, T. Kawaguchi, S. Kuroshima, O. Zhou, *Phys. Rev. B* **1999**, *60*, 13245–13248; b) W. Carrillo-Cabrera, S. Budnyk, Y. Prots, Y. Grin, *Z. Anorg. Allg. Chem.* **2004**, *630*, 2267–2276.
[15] F. Dubois, T. F. Fässler, *J. Am. Chem. Soc.* **2005**,*127*, 3264–3265.
[16] Supporting Information S4: Electron diffraction pattern of the zone axis [100].
[17] Supporting Information S5: Resistivity of $K_7B_7Si_{39}$ vs. temperature.
[18] O. Jepsen, O. K. Andersen, **1999**, TB-LMTO-ASA. Version 4.7. Max-Planck-Institut für Festkörperforschung, Stuttgart, Germany.
[19] Supporting Information S6: Crystallographic data of $K_7B_7Si_{39}$; Supporting Information S7: Atomic coordinates and displacement parameters of $K_7B_7Si_{39}$.
[20] L. G. Akselrud, P. Yu. Zavalii, Yu. Grin, V. K. Pecharsky, B. Baumgartner, E. Wölfel, *Mater. Sci. Forum* **1993**, *133–136*, 335–340.
[21] P. A. Stadelmann, *Ultramicroscopy* **1987**, *21*, 131–145.
[22] N. K. Menon, O. L. Krivanek, *Microsc. Microanal.* **2002**, *8*, 203–215.

